ACS OMEGA

http://pubs.acs.org/journal/acsodf

Article

A Novel Green Approach to Synthesize Curcuminoid-Layered Double Hydroxide Nanohybrids: Adroit Biomaterials for Future Antimicrobial Applications

Chamalki Madhusha, Kumudu Rajapaksha, Imalka Munaweera, Madhavi de Silva, Chandani Perera, Gayan Wijesinghe, Manjula Weerasekera, Dinesh Attygalle, Chanaka Sandaruwan, and Nilwala Kottegoda*

Cite This: *ACS Omega* 2021, 6, 9600−9608

Read Online

ACCESS | Metrics & More | Article Recommendations | Supporting Information

ABSTRACT: Thermal instability, photodegradation, and poor bioavailability of natural active ingredients are major drawbacks in developing effective natural product-based antimicrobial formulations. These inherited issues could be fruitfully mitigated by the introduction of natural active ingredients into various nanostructures. This study focuses on the development of a novel green mechanochemical synthetic route to incorporate curcuminoids into Mg-Al-layered double hydroxides. The developed one-pot and scalable synthetic approach makes lengthy synthesis procedures using toxic solvents redundant, leading to improved energy efficiency. The hydrotalcite-shaped nanohybrids consist of surface and interlayer curcuminoids that have formed weak bonds with layered double hydroxides as corroborated by X-ray diffractograms, X-ray photoelectron spectra, and Fourier transmission infrared spectra. The structural and morphological properties resulted in increased thermal stability of curcuminoids. Slow and sustained release of the curcuminoids was observed at pH 5.5 for a prolonged time up to 7 h. The developed nanohybrids exhibited zeroth-order kinetics, favoring transdermal application. Furthermore, the efficacy of curcuminoid incorporated LDHs (CC-LDH) as an anticolonization agent was investigated against four wound biofilm-forming pathogens, *Pseudomonas aeruginosa*, *Staphylococcus aureus*, methicillin-resistant *Staphyloccocus aureus*, and *Candida albicans*, using a broth dilution method and an *in vitro* biofilm model system. Microbiological studies revealed a 54−58% reduction in biofilm formation ability of bacterial pathogens in developed nanohybrids compared to pure curcuminoids. Therefore, the suitability of these green-chemically synthesized CC-LDH nanohybrids for next-generation antimicrobial applications with advanced dermatological/medical properties is well established.

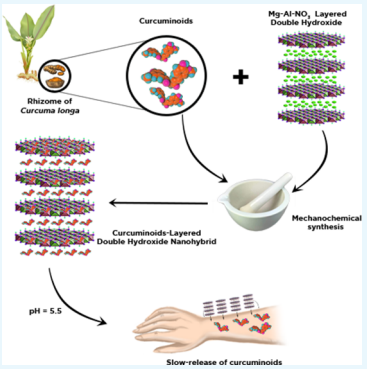

1. INTRODUCTION

Layered double hydroxides (LDHs) are a class of superior host compounds that are capable of intercalating a wide range of guest ions. Their unique structural characteristics derived from the arrangement of layers of the brucite-like structure, which has a general formula of $[M^{II}_{1-x}M^{III}_{x}(OH)_2]_x + (A^{n-})_{x/n}{\cdot}yH_2O$ where M^{II} is a divalent metal ion, M^{III} is a trivalent metal ion, and A^{n-} is an anion, have enabled them to find many practical applications in biomedical fields,[1] catalysis,[2] polymer industry,[3] and food and agriculture.[4a−c] LDHs and its composites are widely used in controlled drug and nutrient delivery since they can act as a good cargo. In these attempts, besides anionic inorganic guests, drug macromolecules and unstable organic molecules derived from biological extracts have been successfully intercalated in LDH in order to obtain stability of guest molecules and slow-release properties. Although there had been many previous attempts to synthesize drug/nutrient-intercalated LDHs hybrids for controlled release, only few research articles are available on intercalation/incorporation of natural active compounds in LDH.[5] Sasaki et al. have successfully intercalated natural α-, β-, and γ-cyclodextrins into Mg-Al-LDH via the calcination−rehydration reaction pathway.[6] Perera and co-workers have successfully synthesized an antifungal formulation using citrate intercalated LDH by a co-precipitation method.[7] Attempts to stabilize curcumin derived from *Curcuma longa* have also been reported by many research groups.[8]

Out of the many potential natural drug molecules that could be stabilized within the layers of LDH and thus used as controlled release drug formulations, curcuminoid intercalated LDH has shown promising applications in the cosmeceutical and pharmaceutical industry.[9] Curcuminoids, a polyphenolic compound extracted from the rhizome of *C. longa*, have

Received: January 10, 2021
Accepted: March 17, 2021
Published: March 30, 2021

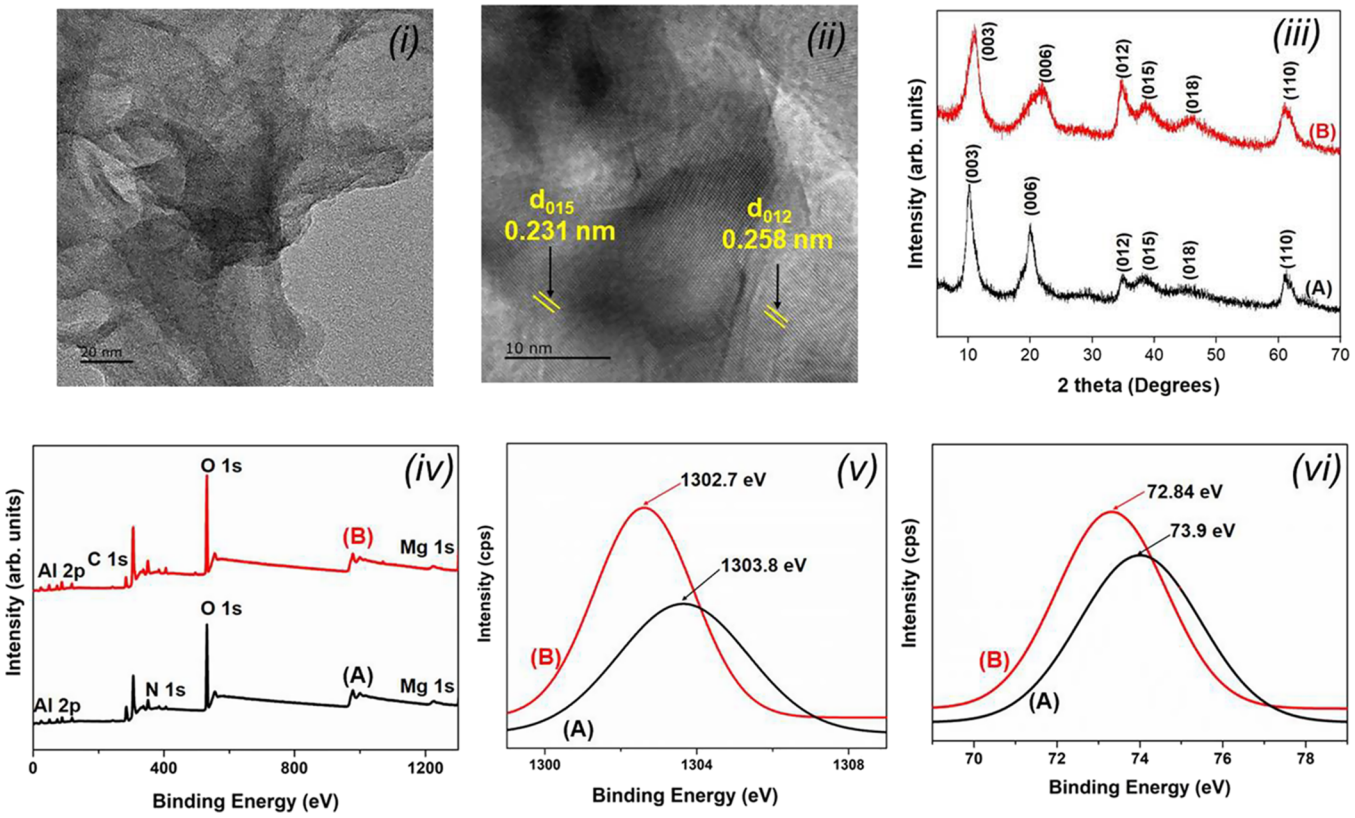

Figure 1. (i) TEM and (ii) HRTEM images of CC-LDH nanohybrids. (iii) PXRD, (iv) full XPS, and (v) Mg 1s and (vi) Al 2p core−shell level of (A) LDH and (B) CC-LDH.

numerous functional properties such as antioxidant, anti-inflammatory, and skin lightening agents, without side effects.[10] However, poor water solubility and stability of curcuminoids due to photodegradation and enzymatic degradation have limited their practical applications.[11] Out of the few attempts to stabilize curcuminoids into LDH, Megalathan et al.[8c] and Samindra and Kottegoda have reported the extraction of curcuminoids using acetone followed by intercalation into Mg-Al-LDH using a co-precipitation approach.[8b] They have studied the structural characteristics of the resulting nanohybrids and also established the release mechanisms of intercalated curcuminoids. In addition, Gayani and co-workers have studied the controlled release properties and their antimicrobial characteristics with reference to the mechanisms involved in the activity of curcuminoid-LDHs.[12]

There are different methods to synthesize LDH, out of which sol−gel synthesis that involves precipitation at a basic pH followed by hydrothermal synthesis has been commonly adopted.[13] In addition, the ion exchange approach, calcination method, and rehydration method have also been exploited for guest anions that have a lesser affinity toward the layers.[14] However, all reported methods have their inherent drawbacks due to the need for carrying out an exothermic reaction at the solution phase. As a result, the processes are lengthy and time-consuming and generate large volumes of waste materials. It is also noteworthy that these preparatory methods lead to low yields due to extensive washing and filtration and in particular low affinity toward the layers when large organic macromolecules are intercalated.[15]

Water-assisted mechanochemical grinding is a common synthesis approach in the drug-developing industry. Although it is a facile method to synthesize LDH too, only a few literature studies are available on the synthesis of large macromolecules' respective anion intercalated LDH.[16] Mechanochemical preparation of LDH is cost-effective compared to the other methods since it does not require heating, inert atmospheres, and solvents as in the traditional methods, and as a result, it allows obtaining LDHs within a short reaction time.[17] This method is also a facile method to force intercalation of macromolecules that are poorly water-soluble and have a lower affinity toward the layers. Moreover, this water-assisted mechanochemical grinding method uses a lower amount of water, thus making this approach more attractive and economical. Briefly, it leads to an easily scalable cleaner reaction with selective intercalation potential for guest molecules.

In our previous study,[8c] we have demonstrated the antimicrobial potential of curcumin intercalated LDH prepared by a co-precipitation approach. Herein, we report a relatively greener, energy-efficient synthesis of naturally extracted curcuminoid incorporated layered double hydroxide nanohybrids via a water-assisted mechanochemical grinding pathway. LDH plays a dual role by enhancing the stability of curcuminoids and acting as a delivery vehicle for the slow, precise, and sustained release of curcuminoids for prolonged periods.[8b] The increased stability and slow release of curcuminoids in CC-LDH nanohybrids exhibit excellent antimicrobial properties.[8c]

2. RESULTS AND DISCUSSION

Morphological, structural, and behavioral patterns of the synthesized CC-LDH nanohybrids were evaluated to establish

https://doi.org/10.1021/acsomega.1c00151
ACS Omega 2021, 6, 9600−9608

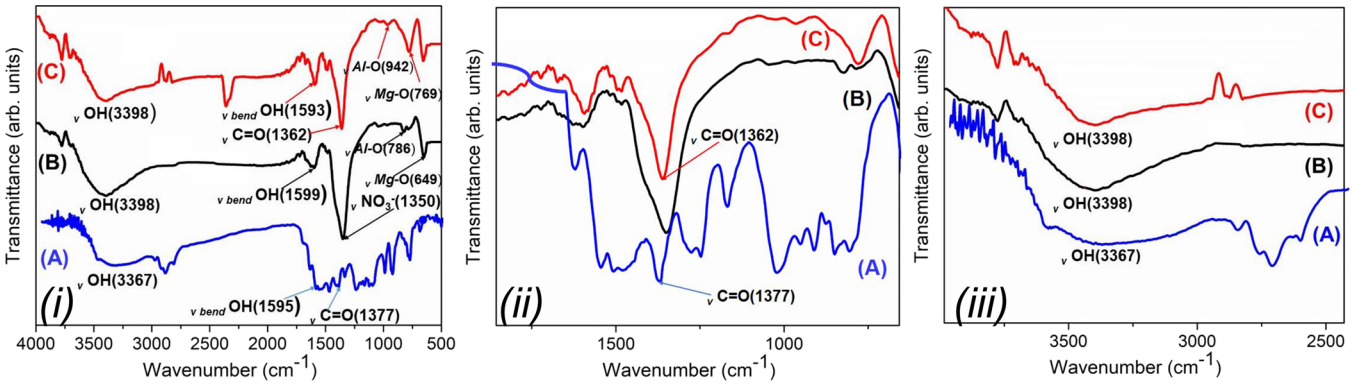

Figure 2. (i) Full FTIR spectra, (ii) carbonyl stretching region, and (iii) OH stretching region of (A) curcuminoids, (B) LDH, and (C) CC-LDH.

the structure−property relationships and investigate the suitability of nanohybrids as a futuristic antimicrobial material. First, the successful extraction of curcuminoids from natural turmeric powder was confirmed by thin-layer chromatography (see Figure S1), indicating the presence of three curcuminoids, namely, curcumin, demethoxycurcumin, and bisdemethoxycurcumin, in the extract.[18] Furthermore, it was determined that the percentage yield of total curcuminoids from *C. longa* extracts was 5.40 ± 0.48% (w/w).

Transmission electron microscopy images revealed that the CC-LDH nanohybrids possess a hydrotalcite-like morphology, as depicted by Figure 1. The interlayer distances along the (015) and (012) planes originating from the LDH were observed at 2.31 and 2.58 Å, respectively. Noteworthily, these mechanochemically synthesized nanohybrids exhibited increased crystallinity comparative to the previously reported curcumin/curcuminoid-encapsulated nanohybrids via co-precipitation synthetic routes.[8c] This elevation in crystallinity awards these CC-LDH nanohybrids better slow-release properties.[8b]

The PXRD patterns (Figure 1(iii)) provided evidence that the structural modifications especially pertaining to the interlayer distances have taken place upon the incorporation of curcuminoids to layered double hydroxides. Even though the appearance of new peaks was not observed, a peak shift of 1.02° was observed at the basal peak corresponding to the (003) plane in the CC-LDH nanohybrid. The original *d*-spacing value of 8.90 Å reported for the Mg-Al-NO_3-LDH of the (003) plane has been reduced to 7.66 Å in the CC-LDH nanohybrid. These values are in good agreement with the previously reported basal spacing for Mg-Al-NO_3-LDH and CC-LDH.[19] This decrease in the interlayer distance results from the strong interactions arising between the phenolic functional groups of curcuminoids and the hydroxyl layers of LDH and aligns with the values from the antecedent work.[8b] It was observed that two different modes of interactions have been established between LDH and curcuminoids. During the synthesis, when strong mechanical forces are applied, the nitrate ions originally present in the LDH are driven out of the layers and the basic pH medium facilitates the keto−enol tautomerism, leading to the formation of negatively charged curcuminoid structures. As a consequence, curcuminoids have the opportunity to move in between the layers of the LDH. The remaining curcuminoids bind from the sides of the layers, which results in further reduction of the interlayer spacing.

The successful replacement of nitrate ions by curcuminoids was further confirmed by XPS analysis with the absence of nitrogen peaks in the spectra (Figure 1(iv)). The changes in the chemical environment around Mg^{2+} and Al^{3+} ions in LDH upon the introduction of curcuminoids were evident from the shifting of Mg 1s and Al 2p peaks to higher binding energy (Figure 1(v),(vi)). These shifts account for the ion−ion electrostatic interactions between Mg^{2+} and Al^{3+} ions present in the LDH with curcuminoid ions, which result in the decrease in electron density around Mg^{2+} and Al^{3+} due to the induction of weak electrostatic shielding. These shifts in Mg^{2+} and Al^{3+} ions are observed in previously reported mechanochemical ground ascorbic acid-intercalated LDH, and the obtained results are compatible.[4] The significant shift in full width at half-maximum (FWHM) values of CC-LDH compared to that of LDH further represents the chemical state changes and physical influences from the external environment such as changing of surface charges, whereas the broadening of a peak indicates the presence of various modes of bonding with varying strengths.[20] XPS quantitative results for the nitrate-LDH and CC-LDH are provided in Table S1 in the Supporting Information.

FTIR analysis data also encouraged the formation of new bonds between curcuminoids and LDH (Figure 2). A cogent peak shift of 29 cm^{-1} was observed in the O−H stretching at 3398 cm^{-1} in the CC-LDH followed by peak broadening. This blue shift in the −OH group is reported in previous CC-LDH, which was prepared in a co-precipitation route.[8a] These changes have been brought by the newly formed H bonds between the hydroxyl groups of curcuminoids and metal hydroxides and interlayer water molecules. Additionally, the peak shifts in the −OH bending regions of CC-LDH also support the formation of H bonds.[21] The carbonyl stretching peak has shifted by 15 cm^{-1} to a lower wavelength in the nanohybrid, indicating the reduction of electron density around an oxygen atom due to the emanation of H bonds with LDH layers and intermolecular water molecules. The Mg-O-H stretching peak and Al-O-H stretching peak also showed FTIR peak shifts as a result of forming H bonds. These metal-oxygen stretchings are specific in LDH, and the obtained values for metal-oxygen stretchings are well aligned with the previously reported FTIR spectra of CC-LDH.[4] The appearance of a new peak at 815 cm^{-1} was observed in the FTIR spectra of CC-LDH corresponding to the metal-oxygen stretching vibrations originating from interactions between curcuminoids and the Mg-Al-layered double hydroxide structure.[22] Assignment of functional groups in FTIR is further illustrated in Table S2.

https://doi.org/10.1021/acsomega.1c00151
ACS Omega 2021, 6, 9600−9608

Thermogravimetric studies unveiled that the thermal stability of curcuminoids has been elevated by virtue of incorporation into LDH (Figure 3). The TGA curve of CC-

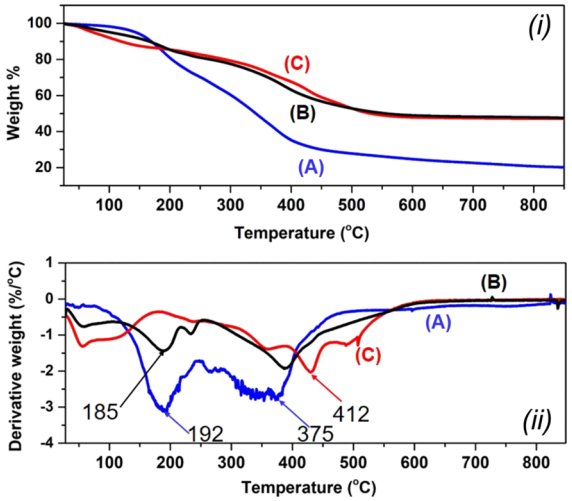

Figure 3. (i) TGA and (ii) DTA of (A) curcuminoids, (B) LDH, and (C) CC-LDH.

LDH showed 7.5% weight loss around 100 °C and 8.1% weight loss around 200 °C corresponding to the removal of physisorbed and chemisorbed water, respectively. These weight loss percentages are well aligned with the previously reported thermograms of LDH.[4] The presence of curcuminoids has helped in reducing the degree of hydration, resulting in only a 15.6% weight reduction below 200 °C. The complete dehydroxylation of the nanohybrid accounted for a 5.1% weight loss within a temperature range of 200−400 °C. Importantly, the complete decomposition of the CC-LDH occurred at 412 °C, which escalated the decomposition temperature of curcuminoids by 37 °C, exhibiting the thermal stabilization of curcuminoids in the presence of LDH matrix. This enhancement of thermal stability makes CC-LDH nanohybrids an excellent candidate in developing novel antimicrobial formulations with increased shelf life and manufacturing stability.

The successful incorporation of curcuminoids into the nanolayers of the LDH was further expressed by the increase in the particle size of CC-LDH to 604 nm while pure nitrate-LDH showed a particle size of 125 nm. However, it should be noted that LDHs are two-dimensional materials possessing morphology of macroplates with nanosize thickness. In such structures, the particle size measurements obtained from dynamic light scattering experiments do not confirm the real size of the materials as they depend on the hydrodynamic radius of the material assuming the spherical shape of a solid particle.[23] Therefore, it is unfair to determine the size of the CC-LDH based only on the particle size measurements. Additionally, transmission microscopy images, which were discussed earlier (Figure 1(i),(ii)), clearly showcase the nanosize interlayer distances. The elevation of the polydispersity index from 0.227 in nitrate-LDH to 0.578 in CC-LDH clearly indicates the emergence of heterogeneity[24] with the introduction of curcuminoids into the LDH structures (Table 1).

The zeta potential of the nitrate-LDH was recorded as 34.7 mV, showing its higher stability[23] in a colloidal suspension.

Table 1. Particle Size, Polydispersity Index, and Zeta Potential of Nitrate-LDH and CC-LDH

parameter	nitrate-LDH	CC-LDH
size (nm)	125	604
polydispersity index	0.227	0.578
zeta Potential (mV)	34.7	−23.1

However, CC-LDH showed moderate stability[23] with a reduced zeta potential of −23.1 mV. This is due to the increase in ionic strength of the dispersion medium originating from the presence of charged molecules like hydroxyl groups (−OH). This can be attributed to the formation of negative charges during the keto−enol tautomerism at the intercalation of curcuminoids and the presence of surface hydroxyl groups in curcuminoids. However, the conclusion of the stability of the nanohybrids should not solely be derived from their colloidal stability as it does not provide a complete view of the stability of materials due to the exclusion of factors like van der waals forces and steric interactions.[24]

The slow, precise, and sustained release of curcuminoids at pH 5.5 was disclosed by the release behavioral studies demonstrating the appropriateness of CC-LDH nanohybrids as an advanced material in developing novel antimicrobial applications (Figure 4). Curcuminoids present on both the surface and interlayers and are weakly bound to LDH gradually release out in a slow-release manner up to 7 h. This release behavior will be advantageous over conventional materials. Kinetic modeling suggested that the release patterns of CC-LDH fit the zeroth-order kinetic model with a 0.99 R^2 value, representing that the release of curcuminoids is a function of time and the rate of release does not depend on the concentration of curcuminoids. The obtained kinetic results are well aligned with the release of curcuminoids from CC-LDH synthesized from the co-precipitation method.[8c] These kinetic properties of CC-LDH nanohybrids are well suited for transdermal delivery systems, making them an ideal candidate for developing skin-care formulations.[25]

Bacterial and fungal skin infections are one of the most prevalent types of infections in developing countries[26] that may lead to serious health issues including sepsis, endocarditis, etc. *Pseudomonas aeruginosa*, *Staphyloccocus aureus*, methicillin-resistant *Staphyloccocus aureus* (MRSA), and *Candida albicans* are four major etiological agents of microbial skin infections,[27] especially in patients with predisposing factors like uncontrolled diabetes mellitus, surgical wounds, suppressed immunity, poor hygiene, and extremes of age.[28] Biofilms are surface-attached microbial aggregates embedded in a self-produced extracellular matrix. This microbial phenotype exhibits more resistance to available antimicrobial agents compared to its free-floating planktonic phenotype.[29] The current study further evaluates the efficacy of CC-LDH nanohybrids as an antimicrobial and antibiofilm agent against common human skin colonizers, *P. aeruginosa*, *S. aureus*, MRSA, and *C. albicans*. Table 2 shows the minimum inhibitory and minimum bactericidal/fungicidal concentrations of CC-LDH and pure curcumin determined using the *in vitro* broth macro dilution method.

Curcuminoids exhibited a ≤10.0 mg/mL MIC value and ≤40 mg/mL bactericidal or fungicidal concentration against all four test strains, whereas CC-LDH exhibited a 40.0 mg/mL MIC value. CC-LDH did not show any bactericidal/fungicidal activity on test organisms at any concentration tested. Based

https://doi.org/10.1021/acsomega.1c00151
ACS Omega 2021, 6, 9600−9608

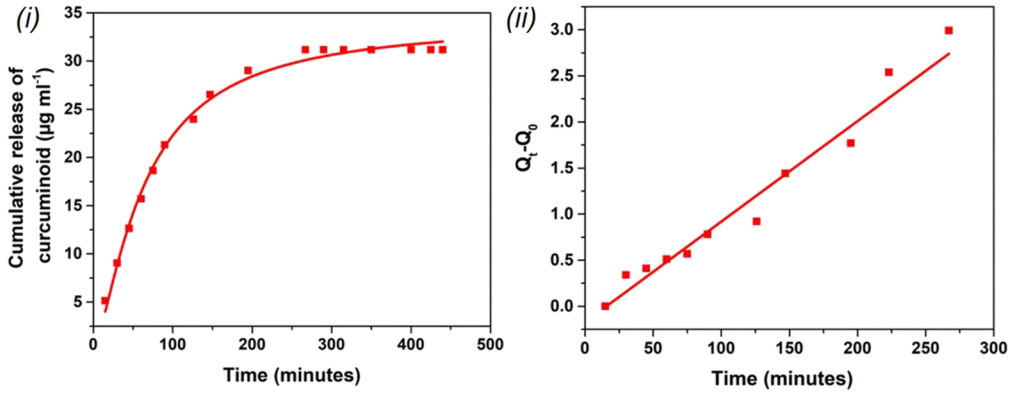

Figure 4. (i) Release profiles of curcuminoids from CC-LDH at pH 5.5 under ambient conditions and (ii) best linear fit (zeroth-order model) of the release of curcuminoids

Table 2. MIC and MBC (or MFC) Values of Pure Curcumin and CC-LDH for the Four Test Strains *P. aeruginosa*, *S. aureus*, MRSA, and *C. albicans*

	treatment (mg/mL)			
	Curcuminoids		CC-LDH	
organism	MIC	MBC or MFC	MIC	MBC or MFC
P. aeruginosa (ATCC 27853)	10.0	40.0	40.0	no MBC point
S. aureus (ATCC 25923)	5.0	20.0	40.0	no MBC point
MRSA	5.0	20.0	40.0	no MBC point
C. albicans (ATCC 10231)	10.0	40.0	40.0	no MFC point

Table 3. Percentage Reduction of the Viability of Developing of Biofilms of *P. aeruginosa* (ATCC 27853), *S. aureus* (ATCC 25923), MRSA, and *C. albicans* (ATCC 10231) in the Presence of 10.0, 25.0, and 50.0 mg/mL Treatment (Compared to Negative Control)

	treatment (mg/mL)					
	Curcuminoids			CC-LDH		
organism	10.0	25.0	50.0	10.0	25.0	50.0
P. aeruginosa (ATCC 27853)	49%	71%	76%	13%	30%	60%
S. aureus (ATCC 25923)	37%	55%	70%	12%	34%	70%
MRSA	12%	42%	59%	7%	24%	53%
C. albicans (ATCC 10231)	5%	56%	70%	6%	17%	71%

on the classification of antimicrobial potency of natural products published by Aligiannis et al.,[30] Curcuminoids show weak antimicrobial activity on test strains. Furthermore, curcuminoids exhibited a bactericidal effect on test strains according to criterion published by Krishnan et al.[31] Importantly, CC-LDH possesses bacteriostatic activity on *P. aeruginosa*, *S. aureus*, MRSA, and *C. albicans*.

Biofilm prevention and control at the early stages of biofilm accumulation are very important since mature biofilms are more resistant than initial immature biofilms[32] and this high resistance of microbial biofilms to routine antimicrobial therapeutics causes serious clinical outcomes such as treatment failure, prolonged hospitalization, or even mortality when the treatment and control of biofilm-associated infections are the concern.[33] The present study evaluates the efficacy of CC-LDH and pure curcumin on controlling the biofilm development of *P. aeruginosa*, *S. aureus*, MRSA, and *C. albicans*. Percentage reduction of the viability of developing microbial biofilms under the exposure of three concentrations of CC-LDH and curcuminoids determined by MTT viability assay is presented in Table 3.

Both curcuminoids and CC-LDH exhibited a high inhibitory effect on developing microbial biofilms. The 50.0 mg/mL CC-LDH and pure curcumin inhibit *in vitro* biofilm development by >50% compared to the negative control. The 25.0 mg/mL pure curcumin reduces the biofilm development of all test strains except MRSA by 50%. Importantly, both curcuminoids and CC-LDH at 50.0 mg/mL concentration do not show any significant difference in biofilm viability reduction of all test strains. However, both treatments show active biofilm prevention at all tested concentrations.

However, when considering the incorporated amount of curcuminoids into LDH, it was estimated that there is 8.2 mg of curcuminoids present in 100 mg of CC-LDH. Though 50 mg/mL CC-LDH and curcuminoids exhibit the viable biofilm biomass reduction of developing microbial biofilms by similar percentages, CC-LDH achieves >50% reduction of viability with low concentrations of the active compound, curcumin. It emphasizes that CC-LDH expresses a similar biological effect (depletion of the biofilm development) by producing low curcuminoid concentration in the medium (around 4.2 mg/mL) for a prolonged period compared to pure curcumin.

SEM images of biofilms of MRSA (clinical isolate) and *C. albicans* (ATCC 10231) developed under the chemical stress of CC-LDH and pure curcumin are shown in Figure 5. SEM images clearly demonstrate cell wall damages, cellular shrinkages, cell wall abnormalities, leakages of intracellular components, and importantly reduction of biofilm cell mass. These observations are in agreement with previously published data by various scientists on the membrane-active nature of curcumin.[12] However, most importantly, the magnitude of cellular destruction and extent of cell density reduction are higher in biofilms formed with CC-LDH treatment compared to biofilms formed with the presence of pure curcumin. We have studied the cytotoxicity of curcuminoids and CC-LDH toward mammalian cells by exposing them to the normal lung cell line MRC-5.[12] This study revealed that curcuminoids show relatively high cytotoxicity compared to CC-LDH where the cytotoxic effect of CC-LDH onsets later at 72 h and is more than 17 times lower than the LD50 of curcuminoids.

https://doi.org/10.1021/acsomega.1c00151
ACS Omega 2021, 6, 9600−9608

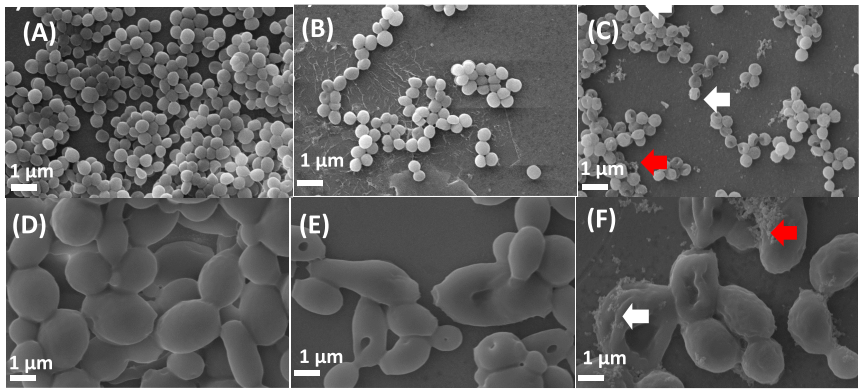

Figure 5. SEM images of the biofilms of (A−C) MRSA and (D−F) *C. albicans* formed with the presence of 10.0 mg/mL pure curcumin and CC-LDH. (A, D) Negative control biofilms. (B, E) Biofilms developed with curcuminoids. (C, F) Biofilms developed with CC-LDH. White solid arrows: leakages of intracellular components. Red solid arrows: cell wall deformities/shrunk cell envelop.

The antimicrobial properties exhibited by CC-LDH have originated from curcuminoids bearing amphipathic and lipophilic properties. Curcuminoids can disturb the cell wall and cell membrane integrity by acting on membrane-associated proteins and phospholipids.[34] This causes alterations in cell membrane permeability and cellular transportation systems, which ultimately lead to cytoplasmic leakages and microbial cell death.[35] At the same time, curcuminoids inhibit the microbial cell division by attaching to structural protein tubulins, which may cause the reduction of the cell densities of treated biofilms.[36]

Furthermore, curcuminoids can interrupt protein synthesis and cellular enzymes by disrupting RNA associated with microbial metabolism.[37] Not only that, natural curcuminoids exhibit a downregulating effect on gene expression of bacteria and inhibition of DNA damage responses, and importantly, these DNA−curcuminoid interactions are the basis of the bacteriostatic effect of curcuminoids.[38]

The ability to reduce the pathogenic biofilm formation shown by CC-LDH is due to the interference of curcuminoids with the intercellular communication system, which facilitates community behaviors and biofilm establishment of microbial pathogens. Biofilm formation is a complex and dynamic process that involves four major steps including adhesion to host surfaces, biofilm maturation, and dispersion of planktonic cells to form microcolonies in distal sites.[39] By interrupting the signal transduction pathways, curcuminoids inhibit the adhesion and biofilm development of microbial pathogens without causing microbial cell death. Additionally, it reduces the biomass and the structural stability of the biofilm.

Even though pure curcuminoids demonstrate a good antimicrobial activity, its instability causes implications in the practical usage in medical applications. The increased stability and the extended release of the active antimicrobial compound, curcuminoids, by the CC-LDH can maximize the therapeutic efficacy of the antimicrobial agent while minimizing the occurrence of antimicrobial resistance.

3. EXPERIMENTAL SECTION

3.1. Materials. All chemicals and reagents in the analytical grade were purchased from Sigma Aldrich, USA. and were used as received. Commercially available natural turmeric powder was used to extract curcuminoids. Distilled water was employed for sample preparations.

3.2. Extraction and Identification of Curcuminoids. Curcuminoids were extracted from natural turmeric powder according to the method reported by Kwon and Chung.[18] Extracted curcumin was analyzed by thin-layer chromatography with a chloroform:methanol (95:5) solvent system as the mobile phase.

3.3. Preparation of Curcuminoid-LDH (CC-LDH) Nanohybrids. First, Mg-Al-NO_3 LDH was synthesized by following the mechanochemical synthetic route described by Ay et al.[17] To the synthesized Mg-Al-NO_3 LDH (1 g) in a ceramic mortar were added extracted curcuminoids powder (6.0 g), NaOH pellets (2.8 g), and water (3 mL) and were ground manually using a ceramic pestle for 1.5 h at room temperature under an inert environment in a glove box. The resultant paste was washed thrice with distilled water (20 mL) and dried at 90 °C to obtain CC-LDH nanohybrids.

3.4. Characterization. The morphology of the synthesized nanohybrids was analyzed with a JEOL JEM-2100 transmission electron microscope. In order to establish structure−property relationships, structural characteristics were studied via several techniques. Powder X-ray diffraction (PXRD) patterns were recorded over a 2-theta angle of 4°−70° at a step size of 0.02° with Cu Kα radiation in a Rigaku-Ultima lV X-ray diffractometer. A Thermo Fisher Scientific X-ray photoelectron spectrometer with a 165 mm ESCALAB Xi+ hemispherical electron energy analyzer with monochromatic Al Kα X-rays was used to obtain X-ray photoelectron spectra. Fourier transform infrared (FTIR) spectral analysis was performed with a Bruker Vertex 80 FTIR spectrophotometer in diffuse reflection mode within a wavelength range of 600−4000 cm^{-1}. The thermal stability of nanohybrids was investigated via a TA Instruments SDT 650 thermogravimetric analyzer over a temperature range of room temperature to 900 °C under a nitrogen atmosphere at 10 °C/min ramp. A Thermo Scientific GENESYS 10S series UV−Vis spectrophotometer was employed to procure UV−Vis spectra. A Malvern Zetasizer Nano ZS particle size analyzer was used to determine the particle size, zeta potential, and polydispersity index (PDI) of the nanohybrids in water. SEM characterization was done using the secondary electron mode of an SU6600 microscope.

3.5. Release Behavior of Curcuminoids at pH 5.5. To study the release of curcuminoids from CC-LDH under simulated conditions equal to human skin, a synthesized phosphate buffer of pH 5.5 was utilized. CC-LDH powder (100 mg) was dispersed in the buffer solution (100.0 mL), and

https://doi.org/10.1021/acsomega.1c00151
ACS Omega 2021, 6, 9600−9608

5.0 mL of aliquot was eluted. The release of curcuminoids into the buffer was quantitatively measured at room temperature using the UV−Vis spectrometer at a wavelength of 427 nm.

3.6. Amount of Incorporated Curcuminoids in CC-LDH. Determination of the total amount of incorporated curcuminoids was carried out by dissolving CC-LDH composite (2 g) in ethanol (15 cm^3) and stirring for 12 h. After 24 h, the absorbance of the filtrate was measured using a UV−Vis spectrometer, and the concentration of curcuminoids was determined at a wavelength of 427 nm.[8c]

3.7. Kinetic Modeling. The data resulting from the release behavioral study was fitted into zeroth-order, first-order, Higuchi, Korsmeyer−Peppas, Avrami-Erofe'ev, Elovich, and Freundlich kinetic models to obtain rate constants and R^2 values to establish the release mechanism of curcuminoids from nanohybrids at pH 5.5.[40] Release behavioral kinetic studies and kinetic models used to analyze the release behavior of curcuminoids from CC-LDH and R^2 values of applied kinetic models (Table S3) are provided in the Supporting Information.

3.8. Antimicrobial and Antibiofilm Activity of CC-LDH Nanohybrids. *3.8.1. Microorganisms and Culture Conditions.* *P. aeruginosa* (ATCC 27853), *S. aureus* (ATCC 25923), methicillin-resistant *S. aureus* (MRSA: a clinical isolate), and *C. albicans* (ATCC 10231) cultures were obtained from the Department of Microbiology, Faculty of Medical Sciences, University of Sri Jayewardenepura, Sri Lanka. Stock cultures of bacteria and *Candida* were maintained on Nutrient Agar (NA, Sigma-Aldrich, USA) slants and Sabouraud Dextrose Agar (SDA, Sigma-Aldrich, USA) slants. In order to obtain 24 h fresh microbial cultures, test strains were subcultured on Brain Heart Infusion (BHI) agar plates (Sigma-Aldrich, USA) and incubated at 35 °C for 24 h.

The standard inocula of test strains were prepared by dissolving few colonies obtained from 24 h fresh microbial cultures in BHI broth and adjusting the turbidity of the inoculum by comparing with a 0.5 McFarland scale.

3.8.2. Minimum Inhibitory Concentration (MIC). MIC was determined using the broth dilution methods with modifications. Briefly, the doubling dilutions of nanohybrids and pure curcumin (2.5, 5.0, 10.0, 20.0, 40.0, and 80.0 mg/mL) were prepared in sterile bijou bottles (1 mL of the dilution in sterile BHI). One milliliter of the prepared standard microbial cell suspension in BHI broth was mixed together with the prepared dilutions, and then the bottles were incubated at 37 °C for 24 h. The content of each bottle was visually observed to detect the presence or absence of turbidity after 24 h incubation. The lowest concentration of the treatment without turbidity was considered as the MIC point.[41]

3.8.3. Minimum Bactericidal/Fungicidal Concentration (MBC/MFC). After the above mentioned visual inspection, the content of each bottle was mixed well and 10 μL aliquot was subcultured on BHI agar (bacteria) or SDA (*Candida*) plates. These plates were further incubated at 37 °C for 24 h. The minimum concentration of the treatment with no visual growth on the agar surface after 24 h incubation was considered as the MBC or MFC point.

3.8.4. Effects on Microbial Biofilm Development. A 24-well sterile polystyrene flat-bottom cell culture plate was seeded with 1 mL of standard microbial cell suspensions of each organism followed by incubation at 37 °C for 2 h. The plate was then carefully washed with 2 mL of sterile normal saline, and 1 mL of the prepared dilutions (10.0, 25.0, and 50.0 mg/mL) of the treatments was added separately to the corresponding wells. One milliliter of BHI broth was added to the negative control wells instead of the treatment. The plate was then incubated at 37 °C for 24 h. The extent of biofilm development of the test strains in the presence of different concentrations of the treatments was quantified using the MTT viability assay explained previously by Weerasekera et al.[42]

3.8.5. Electron Microscopy Studies. The ultrastructure of biofilms formed in the presence of different treatment concentrations was evaluated by SEM. Sterile 10 mm glass coverslips were placed at the bottom of the 12-well cell culture cluster separately. Coverslips were then immersed in 1 mL of the prepared standardized microbial cell suspensions and incubated for 2 h at 37 °C.

Then, the remaining cell suspensions were replaced with the treatment (10.0 mg/mL) in sterile BHI (1 mL/well). Coverslips were incubated for 24 h at 37 °C. After incubation, the coverslips with formed biofilms were subsequently washed twice with sterile distilled water. Then, they were transferred to a new 24-well cell culture cluster containing 2.0% glutaraldehyde. After fixing with glutaraldehyde for 24 h, samples were dehydrated in a series of ethanol solutions and air-dried overnight in an incubator followed by sputter coating with gold. Samples were analyzed under 15k magnification and 10 kV voltages.

4. CONCLUSIONS

A novel, slow-release biomaterial was developed by incorporating curcuminoids as an active natural ingredient into layered double hydroxides via an energy-efficient, greener mechanochemical synthetic route. PXRD and FTIR data revealed the successful formation of a CC-LDH nanohybrid. TEM images confirmed the layering pattern of the resulting nanohybrid, while XPS data further confirmed the structural changes and electron density variations that arise when curcuminoids are incorporated into LDH. Furthermore, CC-LDH obtained from the mechanochemical grinding method has better thermal stability in contrast to the isolated curcuminoids due to the strong host−guest interaction involving the hydrogen bonding and electrostatic interactions. More interestingly, CC-LDH can be used as an effective decolonizing agent or biofilm prevention strategy at the early stages of biofilm development, which would be beneficial to pharmaceutical and cosmetic applications. Thus, we can assert the aptitude of curcuminoid-layered double hydroxides as an advanced biomaterial for the development of the next-generation advanced antimicrobial applications.

■ ASSOCIATED CONTENT

Supporting Information

The Supporting Information is available free of charge at https://pubs.acs.org/doi/10.1021/acsomega.1c00151.

(Figure S1) Thin-layer chromatography of extracted curcuminoids; (Table S1) XPS quantitative results for the nitrate-LDH and CC-LDH; (Table S2) assignment of functional groups in FTIR; and (Table S3) kinetic models used to analyze the release behavior of curcuminoids from CC-LDH and R^2 values of applied kinetic models (PDF)

https://doi.org/10.1021/acsomega.1c00151
ACS Omega 2021, 6, 9600−9608

AUTHOR INFORMATION

Corresponding Author

Nilwala Kottegoda − *Department of Chemistry, Faculty of Applied Sciences and Center for Advanced Materials Research (CAMR), Faculty of Applied Sciences, University of Sri Jayewardenepura, Nugegoda 10250, Sri Lanka;* orcid.org/0000-0002-9664-1704; Phone: 0094 2804206; Email: nilwala@sjp.ac.lk

Authors

Chamalki Madhusha − *Department of Chemistry, Faculty of Applied Sciences, University of Sri Jayewardenepura, Nugegoda 10250, Sri Lanka*

Kumudu Rajapaksha − *Department of Chemistry, Faculty of Applied Sciences, University of Sri Jayewardenepura, Nugegoda 10250, Sri Lanka*

Imalka Munaweera − *Department of Chemistry, Faculty of Applied Sciences, University of Sri Jayewardenepura, Nugegoda 10250, Sri Lanka; Instrument Center, Faculty of Applied Sciences, University of Sri Jayewardenepura, Nugegoda 10250, Sri Lanka*

Madhavi de Silva − *Department of Chemistry, Faculty of Applied Sciences and Center for Advanced Materials Research (CAMR), Faculty of Applied Sciences, University of Sri Jayewardenepura, Nugegoda 10250, Sri Lanka;* orcid.org/0000-0003-3263-2953

Chandani Perera − *Department of Chemistry, University of Peradeniya, Peradeniya 20400, Sri Lanka*

Gayan Wijesinghe − *Department of Microbiology, Faculty of Medical Sciences, University of Sri Jayewardenepura, Nugegoda 10250, Sri Lanka*

Manjula Weerasekera − *Department of Microbiology, Faculty of Medical Sciences, University of Sri Jayewardenepura, Nugegoda 10250, Sri Lanka;* orcid.org/0000-0002-8194-2205

Dinesh Attygalle − *Department of Materials Science and Engineering, University of Moratuwa, Katubedda 10400, Sri Lanka*

Chanaka Sandaruwan − *Sri Lanka Institute of Nanotechnology (SLINTEC), Homagama 10206, Sri Lanka;* orcid.org/0000-0001-6102-096X

Complete contact information is available at: https://pubs.acs.org/10.1021/acsomega.1c00151

Author Contributions

N.K. developed the idea, designed the project, and provided leadership for the team. I.M. and C.P. designed and directed the project and manuscript editing and supervised the project. Furthermore, I.M. was involved in PXRD, FTIR, TEM, XPS, TGA/DTA, and SEM analysis and release data analysis. M.D.S. was involved in the data analysis, manuscript writing/editing, graphical visualization, and scientific feedback. G.W. and M.W. were involved in the microbiology experiments. D.A. helped in the biological SEM analysis. C.S. carried out particle size analysis, zeta potential determination, and XPS studies. K.R. carried out TGA/DTA, FTIR, and PXRD data collection and generated the release profile. C.M. carried out the synthesizing experiments, TGA/DTA, XPS, SEM, and TEM analysis, re-synthesized the materials, analyzed release data and kinetic models, and generated the draft of the manuscript. All authors contributed to the manuscript writing, and N.K. finalized the content. Based on the contribution of all authors, it was decided to name C.M. as the first author.

Funding

The project was funded by the Department of Chemistry, University of Sri Jayewardenepura.

Notes

The authors declare no competing financial interest.

ACKNOWLEDGMENTS

Authors acknowledge the Department of Chemistry and Instrument Center, Faculty of Applied Sciences, and Department of Microbiology, Faculty of Medical Science, University of Sri Jayewardenepura, and Sri Lanka Institute of Nanotechnology for the assistance in conducting characterization and microbiological studies. Furthermore, the authors acknowledge Dr. Tharindu Senapathi for the help in manuscript editing and Mr. V.C.P. Vithana of the Department of Microbiology for helping in the microbiology experiments.

ABBREVIATIONS

CC-LDH, curcuminoid-incorporated layered double hydroxides

REFERENCES

(1) (a) Kuthati, Y.; Kankala, R. K.; Lee, C.-H. Layered double hydroxide nanoparticles for biomedical applications: Current status and recent prospects. *Appl. Clay Sci.* **2015**, *112-113*, 100−116. (b) Munaweera, I.; Koneru, B.; Shi, Y.; di Pasqua, A. J.; Balkus, K. J., Jr. Chemoradiotherapeutic wrinkled mesoporous silica nanoparticles for use in cancer therapy. *APL Mater.* **2014**, *2*, 113315.

(2) He, S.; An, Z.; Wei, M.; Evans, D. G.; Duan, X. Layered double hydroxide-based catalysts: nanostructure design and catalytic performance. *Chem. Commun.* **2013**, *49*, 5912−5920.

(3) Costa, F. R.; Saphiannikova, M.; Wagenknecht, U.; Heinrich, G., Layered double hydroxide based polymer nanocomposites. In *Wax Crystal Control· Nanocomposites· Stimuli-Responsive Polymers*, Springer: 2007; pp. 101−168, DOI: 10.1007/12_2007_123.

(4) (a) Madhusha, C.; Munaweera, I.; Karunaratne, V.; Kottegoda, N. Facile Mechanochemical Approach To Synthesizing Edible Food Preservation Coatings Based On Alginate/Ascorbic Acid-Layered Double Hydroxide Bio-Nanohybrids. *J. Agric. Food Chem.* **2020**, *68*, 8962−8975. (b) de Silva, M.; Siriwardena, D. P.; Sandaruwan, C.; Priyadarshana, G.; Karunaratne, V.; Kottegoda, N. Urea-silica nanohybrids with potential applications for slow and precise release of nitrogen. *Mater. Lett.* **2020**, *272*, 127839. (c) Samavini, R.; Sandaruwan, C.; De Silva, M.; Priyadarshana, G.; Kottegoda, N.; Karunaratne, V. Effect of Citric Acid Surface Modification on Solubility of Hydroxyapatite Nanoparticles. *J. Agric. Food Chem.* **2018**, *66* (13), 3330−3337.

(5) Wang, Y.; Zhang, D.; Bao, Q.; Wu, J.; Wan, Y. Controlled drug release characteristics and enhanced antibacterial effect of graphene oxide−drug intercalated layered double hydroxide hybrid films. *J. Mater. Chem.* **2012**, *22*, 23106−23113.

(6) Sasaki, S.; Yokohama, Y.; Aisawa, S.; Hirahara, H.; Narita, E. Intercalation of natural cyclodextrins into layered double hydroxide by calcination−rehydration reaction. *Chem. Lett.* **2005**, *34*, 1192−1193.

(7) Perera, J.; Weerasekera, M.; Kottegoda, N. Slow release antifungal skin formulations based on citric acid intercalated layered double hydroxides nanohybrids. *Chem. Cent. J.* **2015**, *9*, 1−7.

(8) (a) Khorsandi, K.; Hosseinzadeh, R.; Fateh, M. Curcumin intercalated layered double hydroxide nanohybrid as a potential drug delivery system for effective photodynamic therapy in human breast cancer cells. *RSC Adv.* **2015**, *5*, 93987−93994. (b) Samindra, K. M. S.; Kottegoda, N. Encapsulation of curcumin into layered double hydroxides. *Nanotechnology Reviews* **2014**, *3*, 579−589. (c) Megalathan, A.; Kumarage, S.; Dilhari, A.; Weerasekera, M. M.; Samarasinghe, S.; Kottegoda, N. Natural curcuminoids encapsulated in layered double hydroxides: a novel antimicrobial nanohybrid.

Chemistry Central Journal **2016**, *10*, 1−10. (d) Andrei, F.; Vlad, A.; Birjega, R.; Tozar, T.; Secu, M.; Urzica, I.; Dinescu, M.; Zavoianu, R. Hybrid layered double hydroxides-curcumin thin films deposited via Matrix Assisted Pulsed Laser Evaporation-MAPLE with photoluminescence properties. *Appl. Surf. Sci.* **2019**, *478*, 754−761.
(9) Gutiérrez-Gutiérrez, F.; Sánchez-Jiménez, C.; Rangel-Castañeda, I. A.; Carbajal-Arízaga, G. G.; Macías-Lamas, A. M.; Castillo-Romero, A.; Parra-Saavedra, K. J. Encapsulation of curcumin into layered double hydroxides improve their anticancer and antiparasitic activity. *J. Pharm. Pharmacol.* **2020**, *72*, 897−908.
(10) Sharma, O. Antioxidant activity of curcumin and related compounds. *Biochem. Pharmacol.* **1976**, *25*, 1811−1812.
(11) Anand, P.; Kunnumakkara, A. B.; Newman, R. A.; Aggarwal, B. B. Bioavailability of curcumin: problems and promises. *Mol. Pharmaceutics* **2007**, *4*, 807−818.
(12) Gayani, B.; Dilhari, A.; Wijesinghe, G. K.; Kumarage, S.; Abayaweera, G.; Samarakoon, S. R.; Perera, I. C.; Kottegoda, N.; Weerasekera, M. M. Effect of natural curcuminoids-intercalated layered double hydroxide nanohybrid against Staphylococcus aureus, Pseudomonas aeruginosa, and Enterococcus faecalis: a bactericidal, antibiofilm, and mechanistic study. *MicrobiologyOpen* **2019**, *8*, No. e00723.
(13) Prinetto, F.; Ghiotti, G.; Graffin, P.; Tichit, D. Synthesis and characterization of sol−gel Mg/Al and Ni/Al layered double hydroxides and comparison with co-precipitated samples. *Microporous Mesoporous Mater.* **2000**, *39*, 229−247.
(14) Conterosito, E.; Gianotti, V.; Palin, L.; Boccaleri, E.; Viterbo, D.; Milanesio, M. Facile preparation methods of hydrotalcite layered materials and their structural characterization by combined techniques. *Inorg. Chim. Acta* **2018**, *470*, 36−50.
(15) Padma Kumar, P.; Kalinichev, A. G.; Kirkpatrick, R. J. Hydration, swelling, interlayer structure, and hydrogen bonding in organolayered double hydroxides: Insights from molecular dynamics simulation of citrate-intercalated hydrotalcite. *The Journal of Physical Chemistry B* **2006**, *110*, 3841−3844.
(16) Iwasaki, T.; Yoshii, H.; Nakamura, H.; Watano, S. Simple and rapid synthesis of Ni−Fe layered double hydroxide by a new mechanochemical method. *Appl. Clay Sci.* **2012**, *58*, 120−124.
(17) Ay, A. N.; Zümreoglu-Karan, B.; Mafra, L. A Simple Mechanochemical Route to Layered Double Hydroxides: Synthesis of Hydrotalcite-Like Mg-Al-NO3-LDH by Manual Grinding in a Mortar. *Zeitschrift für anorganische und allgemeine Chemie* **2009**, *635*, 1470−1475.
(18) Kwon, H.-L.; Chung, M.-S. Pilot-scale subcritical solvent extraction of curcuminoids from Curcuma long L. *Food Chem.* **2015**, *185*, 58−64.
(19) Tongamp, W.; Zhang, Q.; Saito, F. Mechanochemical route for synthesizing nitrate form of layered double hydroxide. *Powder Technol.* **2008**, *185*, 43−48.
(20) Ratnayake, S. P.; Purasinhala, K.; Sandaruwan, C.; de Silva, Y. M.; Mantilaka, M. M. M. G. P. G.; Priyadarshana, G.; Amaratunga, G. A. J.; de Silva, K. M. N. Combined Zr and Y phosphate coatings reinforced with chemically anchored B2O3 for the oxidation inhibition of carbon fiber. *Materialia* **2021**, *15*, 100984.
(21) Zhang, H.; Zhu, Y.; Sun, X.; He, X.; Wang, M.; Wang, Z.; Wang, Q.; Zhu, R.; Wang, S. Curcumin-loaded layered double hydroxide nanoparticles-induced autophagy for reducing glioma cell migration and invasion. *J. Biomed. Nanotechnol.* **2016**, *12*, 2051−2062.
(22) Islam, M.; Patel, R. Synthesis and physicochemical characterization of Zn/Al chloride layered double hydroxide and evaluation of its nitrate removal efficiency. *Desalination* **2010**, *256*, 120−128.
(23) Bhattacharjee, S. DLS and zeta potential−what they are and what they are not? *J. Controlled Release* **2016**, *235*, 337−351.
(24) Patel, G. K.; Khan, M. A.; Zubair, H.; Srivastava, S. K.; Kushman, M.; Singh, S.; Singh, A. P. Comparative analysis of exosome isolation methods using culture supernatant for optimum yield, purity and downstream applications. *Sci. Rep.* **2019**, *9*, 1−10.
(25) Rungphanichkul, N.; Nimmannit, U.; Muangsiri, W.; Rojsitthisak, P. Preparation of curcuminoid niosomes for enhancement of skin permeation. *Die Pharmazie-An International Journal of Pharmaceutical Sciences* **2011**, *66*, 570−575.
(26) Ramakrishnan, K.; Salinas, R. C.; Higuita, N. I. A. Skin and soft tissue infections. *Am. Fam. Physician* **2015**, *89*, 474−420.
(27) Weller, R.; Price, R. J.; Ormerod, A. D.; Benjamin, N.; Leifert, C. Antimicrobial effect of acidified nitrite on dermatophyte fungi, Candida and bacterial skin pathogens. *J. Appl. Microbiol.* **2001**, *90*, 648−652.
(28) Ramamuthie, G.; Verma, R. K.; Appalasamy, J.; Barua, A. Awareness of risk factors for skin infections and its impact on quality of life among adults in a malaysian city: a cross-sectional study. *Trop. J. Pharm. Res.* **2015**, *14*, 1913−1917.
(29) Maia, F. C.; Wijesinghe, G. K.; de Oliveira, T. R.; Barbosa, J. P.; de Feiria, S. B.; Boni, G. C.; Ramos, M. M. B.; Anibal, P. C.; Höfling, J. F. Phyllanthus niruri L.(stone-breaker) as an alternative of anti-human diseases, antimicrobial agent, and its applicability to combat resistant microrganisms. A Brief Review. *Brazilian Journal of Natural Sciences* **2020**, *3*, 342−342.
(30) Aligiannis, N.; Kalpoutzakis, E.; Mitaku, S.; Chinou, I. B. Composition and antimicrobial activity of the essential oils of two Origanum species. *J. Agric. Food Chem.* **2001**, *49*, 4168−4170.
(31) Krishnan, N.; Ramanathan, S.; Sasidharan, S.; Murugaiyah, V.; Mansor, S. M. Antimicrobial activity evaluation of Cassia spectabilis leaf extracts. *IJP-International Journal of Pharmacology* **2010**, *6*, 510−514.
(32) Percival, S. L.; Salisbury, A.-M.; Chen, R. Silver, biofilms and wounds: resistance revisited. *Critical reviews in microbiology* **2019**, *45*, 223−237.
(33) Wijesinghe, G.; Jayarathne, P.; Gunasekara, T.; Fernando, N.; Kottegoda, N.; Weerasekera, M., *Antibacterial and anti-candida activity of chlorhexidine gluconate, Triphala and Munamal pothu (bark of Mimusops elengi)*. 2018.
(34) Tyagi, P.; Singh, M.; Kumari, H.; Kumari, A.; Mukhopadhyay, K. Bactericidal activity of curcumin I is associated with damaging of bacterial membrane. *PLoS One* **2015**, *10*, No. e0121313.
(35) Barry, J.; Fritz, M.; Brender, J. R.; Smith, P. E. S.; Lee, D.-K.; Ramamoorthy, A. Determining the effects of lipophilic drugs on membrane structure by solid-state NMR spectroscopy: the case of the antioxidant curcumin. *J. Am. Chem. Soc.* **2009**, *131*, 4490−4498.
(36) Rai, D.; Singh, J. K.; Roy, N.; Panda, D. Curcumin inhibits FtsZ assembly: an attractive mechanism for its antibacterial activity. *Biochem. J.* **2008**, *410*, 147−155.
(37) Zheng, D.; Huang, C.; Huang, H.; Zhao, Y.; Khan, M. R. U.; Zhao, H.; Huang, L. Antibacterial Mechanism of Curcumin: A Review. *Chem. Biodiversity* **2020**, *17*, No. e2000171.
(38) Jenkins, H. E.; Tolman, A. W.; Yuen, C. M.; Parr, J. B.; Keshavjee, S.; Pérez-Vélez, C. M.; Pagano, M.; Becerra, M. C.; Cohen, T. Incidence of multidrug-resistant tuberculosis disease in children: systematic review and global estimates. *The Lancet* **2014**, *383*, 1572−1579.
(39) Wijesinghe, G. K.; de Oliveira, T. R.; Maia, F. C.; de Feiria, S. B.; Joia, F.; Barbosa, J. P.; Boni, G. C.; Höfling, J. F. Cinnamomum verum (true cinnamon) leaf essential oil as an effective therapeutic alternative against oral and non-oral biofilm infections: A brief review. *Brazilian Journal of Natural Sciences* **2020**, *3*, 556−556.
(40) Munaweera, I.; Shi, Y.; Koneru, B.; Patel, A.; Dang, M. H.; Di Pasqua, A. J.; Balkus, K. J., Jr. Nitric oxide-and cisplatin-releasing silica nanoparticles for use against non-small cell lung cancer. *J. Inorg. Biochem.* **2015**, *153*, 23−31.
(41) Wikler, M. A. Methods for dilution antimicrobial susceptibility tests for bacteria that grow aerobically: approved standard. *CLSI (NCCLS)* **2006**, *26*, M7−A7.
(42) Weerasekera, M. M.; Jayarathna, T. A.; Wijesinghe, G. K.; Gunasekara, C. P.; Fernando, N.; Kottegoda, N.; Samaranayake, L. P. The effect of nutritive and non-nutritive sweeteners on the growth, adhesion, and biofilm formation of Candida albicans and Candida tropicalis. *Medical Principles and Practice* **2017**, *26*, 554−560.

https://doi.org/10.1021/acsomega.1c00151
ACS Omega 2021, 6, 9600−9608